TRIBHUVAN UNIVERSITY

INSTITUTE OF ENGINEERING

PULCHOWK CAMPUS

THESIS NO: 079MSMSE003

Metal Organic Framework Decorated Hemp Hurd Derived Carbon for Energy Storage Application

by

Gyanendra Pal

A THESIS

SUBMITTED TO THE DEPARTMENT OF APPLIED SCIENCES AND CHEMICAL ENGINEERING

IN PARTIAL FULFILLMENT OF THE REQUIREMENTS FOR THE

DEGREE OF MASTER OF SCIENCE IN MATERIAL SCIENCE AND ENGINEERING

DEPARTMENT OF APPLIED SCIENCES AND CHEMICAL ENGINEERING

LALITPUR, NEPAL

MAY, 2025

COPYRIGHT

TRIBHUVAN UNIVERSITY

INSTITUTE OF ENGINEERING

PULCHOWK CAMPUS

DEPARTMENT OF APPLIED SCIENCES AND CHEMICAL ENGINEERING

The undersigned certify that they have read, and recommended to the Institute of Engineering for acceptance, a thesis entitled **"Metal Organic Framework Decorated Hemp Hurd Derived Carbon for Energy Storage Application"** submitted by Mr. Gyanendra Pal (079MSMSE003) in partial fulfilment of the requirements for the degree of Masters in Material Science and Engineering.

Assistant Professor Dr. Tanka Mukhiya
Supervisor
Department of Applied Sciences and Chemical Engineering,
Institute of Engineering, Pulchowk Campus
Tribhuvan University, Nepal

Professor Dr. Armila Rajbhandari (Nyachhyon)
External Examiner
Central Department of Chemistry
Tribhuvan University, Nepal

Tribhuvan University
Institute of Engineering
Pulchowk Campus
Department of
Applied Sciences and Chemical Engineering

Professor Dr. Sahira Joshi
Head of Department
Department of Applied Sciences and Chemical Engineering
Institute of Engineering, Pulchowk Campus
Tribhuvan University, Nepal

ABSTRACT

This study investigates the preparation of Metal organic Framework-based carbon from hemp hurd and its application for energy storage purpose. The main objective of this study is to prepare nanoporous carbon from hemp hurd powder by MOF modification using Cobalt Nitrate Solution and 2-Methylimidazole. The physicochemical properties of the carbon materials were carried out in terms of x-ray diffraction (XRD), Fourier transform infra-red spectroscopy (FTIR) and Field emission scanning electron microscopy (FESEM). The electrochemical properties of as-obtained carbon were assessed for potential use in supercapacitors. Electrochemical measurements were performed using a three-electrode system with the prepared samples as working electrodes, an Ag/AgCl as a reference electrode, and a platinum as a counter electrode in a 6 M KOH electrolyte. The electrochemical properties were evaluated using cyclic voltammetry (CV), Galvanometric Charging and Discharging (GCD) Analysis and Electrochemical Impedance Spectroscopy (EIS). The CV curves shows that the superior performance of HDMC 900. GCD analysis shows that the specific capacitance of HDMC 900 was 270.47 F g^{-1}. In conclusion, this study highlights the potential uses of hemp hurd based MOF carbon as a sustainable and efficient material for supercapacitor, offering an eco-friendly and low-cost alternative to conventional materials.

Keywords: Hemp hurd, Metal organic framework, Supercapacitor, Carbon, Energy.

ACKNOWLEDGEMENTS

I am very grateful for the invaluable support and guidance I have received throughout this journey.

First and foremost, I would like to extend my sincere appreciation to my esteemed supervisor, Assistant Professor Dr. Tanka Mukhiya, Department of Applied Sciences and Chemical Engineering, Pulchowk Campus. His unwavering encouragement, consistent guidance, and insightful suggestions have been weapon in shaping this work.

I would also like to thank Professor Dr. Sahira Joshi, Head of the Department, and Associate Professor Dr. Ganesh Kumar Shrestha, Programme coordinator, M.Sc. in Materials Science and Engineering and all the staffs of Department of Applied Sciences and chemical Engineering, Pulchowk Campus for their fruitful contributions and valuable suggestions.

I would like to thank Assistant Professor Dr. Deval Prasad Bhattarai, Department of Chemistry, Amrit Campus, for support in providing laboratory facilities and collaboration.

I want to express my deepest gratitude to Assistant Professor. Purnima Mulmi, Mr. Rajesh Shrestha, Mr. Ashman Karki, Ms. Bipana Ojha Khatri for their guidance and help during the lab work.

Lastly, I would like to express my deepest gratitude to my family and friends, for their unwavering assistance, moral support, and encouragement during times of need. Their contributions have been indispensable, and I am truly fortunate to have had their support throughout this journey.

Gyanendra Pal

May, 2025

TABLE OF CONTENTS

LIST OF FIGURES

LIST OF TABLES

LIST OF ACRONYMS AND ABBREVIATIONS

AC	Activated Carbon
CV	Cyclic voltammetry
EDL	Electrostatic double layer
EDX	Energy dispersive X-ray
EIS	Electrochemical impedance spectroscopy
E_p	Peak potential
FESEM	Field emission scanning electron microscopy
FTIR	Fourier Transform Infrared Spectroscopy
GCD	Galvanostatic Charge Discharge
HDC	Hemp hurd MOF Distilled water Carbon
HMC	Hemp hurd MOF Methanolic Carbon
HDMC	Hemp hurd MOF Distilled water and Methanolic Carbon
I_p	Peak current
KHz	Kilohertz
LIBs	Lithium-Ion Batteries
MHz	Megahertz
MOF	Metal organic framework
r.p.m	Revolutions per minute
SEM	Scanning Electron Microscopy
SC	Supercapacitor
TEM	Transmission electron microscopy
Wt %	Weight percentage
XRD	X-ray diffraction
ZIF	Zeolitic imidazolate framework
%	Percentage

Ω	Ohm
°C min^{-1}	Degree Celsius per minute
μm	Micrometer
A g^{-1}	Ampere per gram
°C	Degree Celsius
F g^{-1}	Farad per gram
hrs	Hours
kW kg^{-1}	Kilowatt per kilogram
L	Litre
M	Molar
mAh g^{-1}	Milliampere hours per gram
mV	Millivolt
mW cm^{-2}	Milliwatt per square centimeter
nm	Nanometer
W kg^{-1}	Watt per kilogram
Wh kg^{-1}	Watt-hour per kilogram
Z’	Real impedance
-Z”	Imaginary impedance

CHAPTER 1: INTRODUCTION

1.1 Background

With the advancement in technology day by day it is very essential to develop thin, light and low-cost supercapacitors for various energy storage applications. Moreover, the world is facing climate change and global warming problems due to high usage of fossil fuels, and the use of renewable sources for the development of electronic devices getting appreciations worldwide (Srinivasan et al., 2020). Fossil fuel crisis also leads researchers to think about development of different types of high-performance supercapacitors for their long-life cycle, greater energy storage capacity and high-power density (Guo et al., 2021). Energy storage systems (ESS) help balance supply and demand by storing excess energy during high-generation periods and feeding it back in periods of low production or peak demand. Such a role helps maintain grid stability, improve energy security, and enable the mass deployment of clean energy technologies (Hançer Güleryüz & Özen, 2022).

Beyond that, energy storage devices are also critical in applications requiring instant or reserve power, such as electric vehicles (EVs), medical equipment, and industrial machinery. In EVs, for instance, the combination of high-power density and fast charge-discharge cycles offered by energy storage devices ensures optimum performance and maximum range. Besides, in developing nations or off-grid areas with weak power infrastructure, such devices provide round-the-clock energy access and reduce dependence on fossil-fuel-based backup power generators (Şahin et al., 2022).

Biowaste materials, such as agricultural waste, fruit peels, and plant-based waste, have been excellent precursors for eco-friendly energy storage devices, such as supercapacitors and batteries. These materials are rich in carbon and can be transformed into activated carbon through pyrolysis or chemical activation in order to achieve porous structures with high surface area and moderate electrical conductivity. For instance, banana peel-based activated carbon exhibited excellent electrochemical performance with a specific capacitance (Y. Zhang et al., 2016).

Activated carbon is widely used as gas-phase and liquid phase adsorbent. Its modern manufacturing processes involve carbonization and activation to reach the desired pore structure and mechanical strength. The process of carbonization takes several hours and consumes a lots

of energy to get the desired level of activation (Pullas Navarrete & de la Torre, 2022). Activated carbon fiber is also known as third generation of activated carbon material. It has strong adsorption capacity due to its large specific surface area and can absorb and remove organic matter in water. The heavy metals in terms of environmental pollutions are Mercury, Lead, Cadmium, Chromium, and metalloid arsenic. These metals have great toxic effects on environments and they can be removed from environment by the adsorption method to treat heavy metal containing waste water (Yu et al., 2022). The purpose of carbonization is to reduce the volatile content of raw materials via pyrolysis of the carbon precursors in the temperature range of 300–900 °C and to create char with primary porosity associated with a high content of fixed carbon (Aryal et al., 2025). The purpose of activation is to improve the specific surface area or pore volume of AC by opening new pores and developing the existing pores (Gao et al., 2020).

Fig. 1. (a)Plant of Hemp and (b) Stem of Hemp Extracted

Hemp (Cannabis sativa) is herb dicotyledonous plant generally known as Marijuana, it belongs to order Rosales, family Cannabaceae and genus Cannabis. Application of hemp plant in industrial as well as general uses. Mainly hemp plant is used for production of different products like medicine, clothes, paper, cosmetic materials, oil, beverages and other healthy foods etc. (Liu et al., 2024).

1.2 Metal Organic framework

Metal-Organic frameworks (MOFs) are formed by coordination between metal ions and organic ligands. MOFs are greatly increasing the interest of researchers due to their adjustable pore size, high specific surface area as well as arranged crystal structure, they are widely used in various applications such as supercapacitors, sensors, catalysis and gas adsorption and separation. MOFs materials are made up of Cations and Anions, which helps to increase the conducting capacity of materials as well as charge storage properties (Zhang et al., 2020).

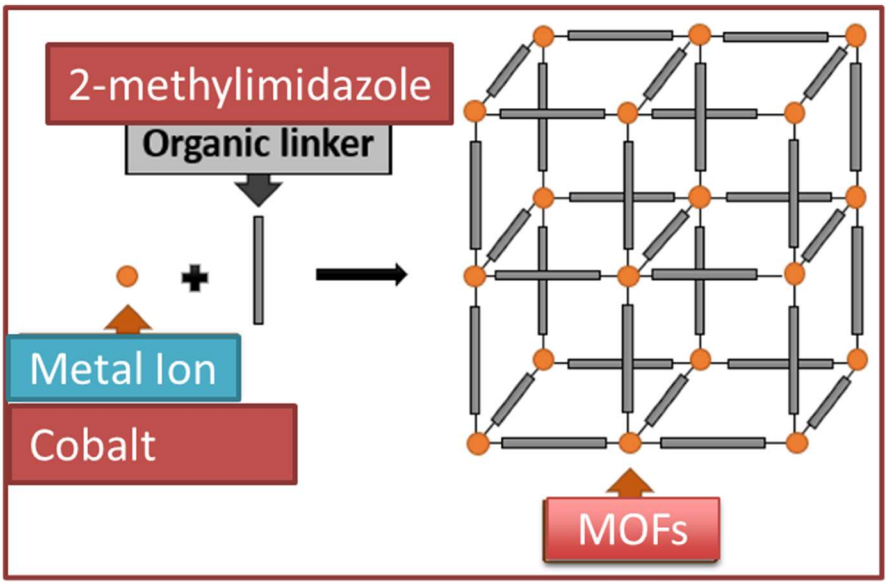

Fig. 2. Components of MOF

MOFs possess crystalline architecture, high surface area, and adaptable pore size. Their remarkable characteristics of metal-organic frameworks (MOFs) and their derivatives, including their structural homogeneity, topology diversification, and adaptability of functionality, have rendered them well known (Mukhiya et al., 2021).

Material scientists in many energy-related fields are highly interested in materials that are fabricated from metal-organic frameworks. Some of these fields include water splitting, oxygen reduction reactions, batteries, photovoltaics, supercapacitors, sensing, drug storage/delivery, hydrogen storage, photoinduced hydrogen evolution, and methane storage (Raoof et al., 2015).

1.2.1 Zeolitic imidazolate framework

Among the broad library of MOFs, there is a distinct subset referred as MOF-zeolitic imidazolate frameworks (ZIFs) which are comprised of transition-metal cations (M) and imidazole-based ligands (Norouzbahari et al., 2023).

These materials offer tunable porosity, framework flexibility, and the potential for functionalizing their internal surfaces. They also have thermal, mechanical, and chemical stability. In ZIFs, imidazolate linkers connect metal centers to yield three- dimensional porous crystalline solids, which have the same shape as traditional inorganic zeolites (Chhetri et al., 2020).

1.3 Supercapacitors

Supercapacitors are intermediate between electrochemical batteries that store large amounts of charges and dielectric capacitors which can deliver huge amount of power during few milliseconds. Super capacitors are mainly three types: Carbon-carbon, metal oxide and electrochemically conducting polymers (Gamby et al., 2001). Petroleum resources are becoming increasingly tight, global warming, environmental pollution is becoming more and more serious. The earth is facing enormous energy challenges. These conditions have forced countries to work towards new sources of sustainable energy and advanced energy storage technologies. There is no alternative renewable source of energy other than solar, water and wind. However, solar is restricted to day and night, season, geographical location, altitude and other conditions. Wind energy collection also requires local wind speed, noise is high and intermittent, and requires the coordination of energy storage devices. Hence Supercapacitor have a wide range of attention as an energy storage devices (He & Zhang, 2022).

1.3.1 Types of Supercapacitors

There are mainly three types of supercapacitor : Electrochemical Double Layer Supercapacitors (EDLC), Pseudo capacitors and lithium-ion Hybrid Supercapacitors (Vondrak et al., 2018). They are shown in **Fig. 3.**

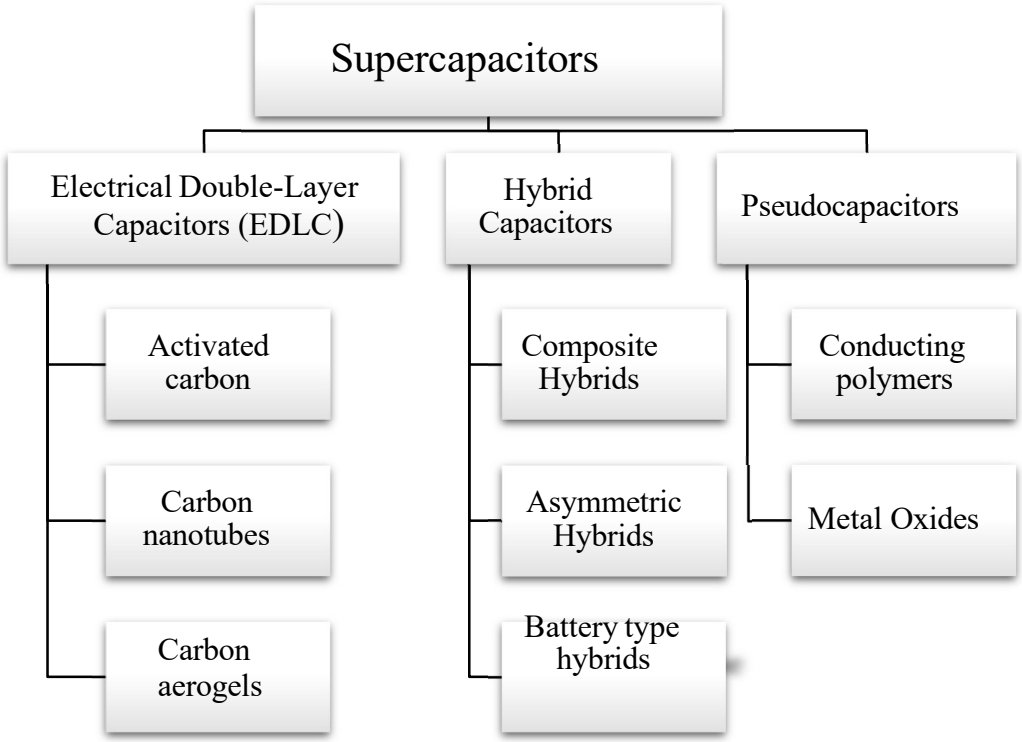

Fig. 3. Types of Supercapacitors

1. Electrochemical Double Layer Supercapacitors (EDLC)

Electric Double Layer Capacitors (EDLC) are a type of supercapacitor that store energy by electrostatic separation of ions at the interface between electrode and electrolyte. EDLCs operate through physical process and enables to achieve extremely fast charging discharging, high power density and longer lifespan (Simon & Gogotsi, 2008).In EDLC type supercapacitors carbon based materials are used for electrodes (Cevher & Çırpan, 2025). In electrical double layer capacitors (EDLCs), energy is stored and released through nanoscale charge separation at the electrochemical interface formed between the electrode and electrolyte. This mechanism of charge storage is non- faradaic, meaning it does not involve chemical oxidation-reduction (redox) reactions. Representative figure of EDLC Supercapacitor is as shown in **Fig. 4**.

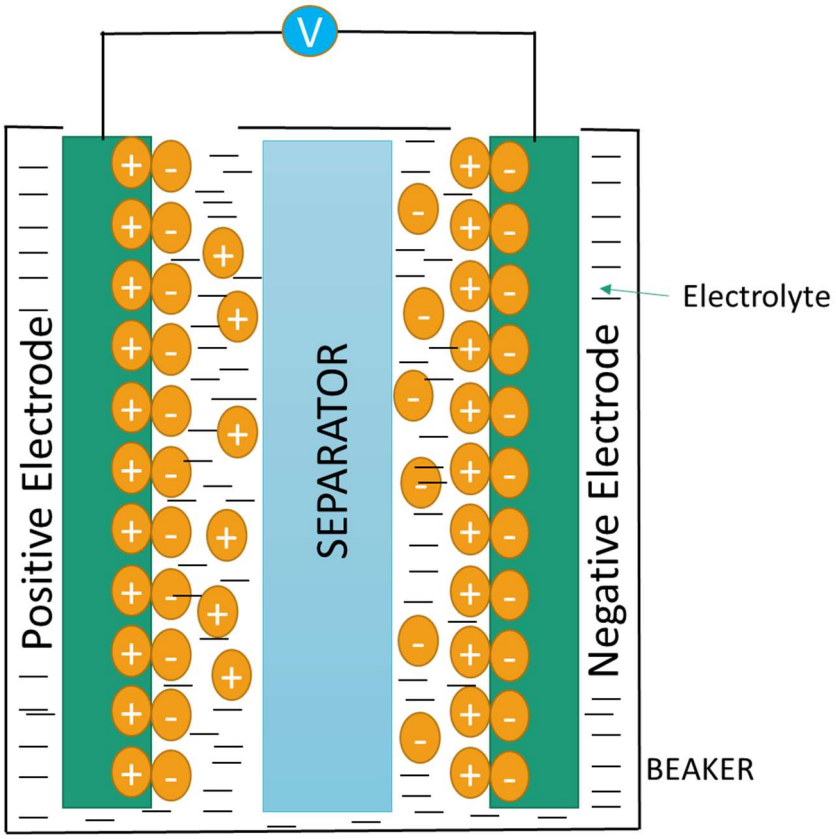

Fig. 4. EDLC Type of Supercapacitor

2. Pseudocapacitors

Pseudo-Capacitors store energy through fast and reversible redox reaction at the electrode surface and generally transition metal oxides-based materials or conducting polymers are used for electrode preparation. They have (Kumar et al., 2022). They have higher capacitance and energy density than EDLC but their life cycle span may be shorter (R. Liu et al., 2021).

3. Lithium-ion Hybrid Supercapacitor

They are prepared from the combination of properties of both EDLC and Pseudo-capacitor or batteries. They are aimed for obtaining high energy and power density. The materials for this type of supercapacitor is carbon materials with metal oxide or lithium ion batteries (Choudhary et al., 2017).

1.3.2 Characteristics of Supercapacitors

Following are the characteristics of Supercapacitor (Libich et al., 2018).

- High Power Density: Supercapacitors possess high power output capability with rapid delivery, which is needed in applications like electric vehicle regenerative braking.
- Low Energy Density: They possess less energy storage than conventional batteries and therefore are not meant for long-duration power supply.
- Fast Charging and Discharging: They can charge and discharge from seconds to minutes, which is suitable for systems requiring fast energy transfer.
- Long Cycle Life: Supercapacitors possess hundreds of thousands to millions of cycles with little loss of capacity in contrast to those batteries with limited lifetimes.
- Broad Operating Temperature Range: They possess good operation over a broad operating temperature range (−40°C to +70°C or better), making them compact and convenient for a broad range of applications.
- Low Equivalent Series Resistance (ESR): Low ESR facilitates efficient operation through minimized energy loss during charging and discharging.
- Environmentally Friendly: The majority of supercapacitors employ harmless materials, showing less environmental risk than regular batteries.

1.3.3 Application of Supercapacitors

Supercapacitors are widely used in electric and hybrid vehicles, renewable energy infrastructure, portable electronic devices, and industrial equipment. They are also used to store energy generated during periods of high production in renewable power systems and discharge it during periods of low production to ensure grid stability. Supercapacitors are also in demand in mobile electronics, where they offer quick charging time and supply power to high-energy-consumption devices like cameras and LED flashlights. (Libich et al., 2018).

1.4 Carbo Nanotubes (CNTs)

Carbon nanotubes (CNTs) are nanostructures in the cylindrical shape made of carbon atoms that are densely packed in a hexagonal arrangement, as seen in graphene sheets rolled into a cylindrical shape. They are characterized by unprecedented mechanical strength, electrical conductivity, and thermal stability, which make them extremely versatile for many applications in energy storage,

electronics, and material science. CNTs are primarily divided into two categories: single-walled carbon nanotubes (SWCNTs) and multi-walled carbon nanotubes (MWCNTs). Due to their high surface area and conductivity, CNTs have been extensively employed in supercapacitors and lithium-ion batteries as electrode materials for enhancing charge storage and cycling stability.(Hu et al., 2019).

1.5 Statement of Problem

The increasing demand for efficient, sustainable, and flexible energy storage devices has led to a surge in research on energy storage. However, conventional energy storage devices are often limited by complex and expensive fabrication methods, reliance on non-renewable materials, and poor long-term mechanical stability. *Hemp*, a naturally abundant and renewable bio resource, presents a promising alternative for the development of eco-friendly and highly porous MOF based hemp hurd carbon. Despite its potential, little research has been conducted on utilizing *MOF based hemp hurd* in energy storage devices.

There is a significant gap in understanding how to optimize the material properties Hemp to achieve high electrochemical performance, durability, and scalability in carbon. This study aims to address these challenges by investigating the suitability of MOF based hemp hurd Carbon for energy storage applications, focusing on improving their structural integrity, electrochemical efficiency, and fabrication process. By doing so, it seeks to contribute to the development of sustainable, high-performance energy storage solutions.

CHAPTER 2: LITERATURE REVIEW

2.1 Literature Review

As lithium-ion batteries have replaced conventional rechargeable batteries such as NiCd or NiMH batteries. And technology is upgrading day by day LIBs have grown to include in electric vehicles and electric energy storage system, beyond this they are useful for portable electronic devices and wearable and flexible IT devices like watches, flexible displays etc. To resolve these problems electrodes with unique structure having flexibility and good performance is essential for LIBs (Park et al., 2017).

As demand of long lasting and high-performance charge storage devices is increasing, the attention of researcher is attracted by bio-based waste materials for the fabrication of electrode materials for Supercapacitor. (Rosas et al., 2009) prepared highly porous carbon materials by chemical activation of hemp fibers. This helps to understand the hemp hurd powder has good electrochemical properties.

(J. Zhang et al., 2016)synthesized Nitrogen and Sulphur Co-doped porous carbon microspheres (NS-PCMSs) with enhanced electrochemical performance for supercapacitors by different Sulphur sources, i.e., sublimed Sulphur, thiourea, and Tetramethyl thiuram disulfide (TMTD), through a solvothermal method. Electrochemical tests revealed that NS-PCMSs exhibited enhanced specific capacitance (242-295 F g-1 at 0.1 A g-1), excellent rate ability (216-247 F g-1 at 10 A g-1), and excellent cyclic stability (almost no attenuation after 10,000 cycles).

(Wang et al., 2020) created a composite Co_3O_4/Carbon aerogels on the basis of ZIF- 67 for application as an electrode for supercapacitors. This was achieved through the method of in- situ deposition followed by calcination. Enhanced electron and ion transfer was facilitated by the unambiguous 3D nanoarchitecture. As a result, the composite electrode exhibited an excellent specific capacitance of 298.8 F g-1 at 0.5 A g-1, along with excellent rate capability and cycling stability that retained 82 % capacity after 1000 cycles. These findings exhibited immense potential for the application of such composite electrodes in electrochemical supercapacitors.

(Yao et al., 2017) also prepared MOF-derived nanoporous carbon (MOF-NPC) by direct calcination of zinc-based MOF at variable carbonization temperatures. Afterwards, MOF-NPC/MnO2 hybrid materials were constructed by a self-controlled redox process with effective

confinement of MnO2 nanostructures within MOF-NPC porous framework. According to these materials, an asymmetric supercapacitor was constructed with MOF-NPC/MnO2 hybrids as the positive electrode and MOF-NPC as the negative electrode in a neutral aqueous Na_2SO_4 electrolyte. The maximized asymmetric cell demonstrated reversible cycling within the range of 0-2.2 V and showed a peak energy density of 76.02 Wh kg-1 (at a power density of 2.20 kW kg-1) and a peak power density of 22.00 kW kg-1 (at an energy density of 49.56 Wh kg-1), which implies its high possibility of being applied in practical energy storage.

More recently, (Minakshi et al., 2024) has reported that the synthesis of highly porous carbon honeycomb structure derived from Australian hemp with chemical activation gives excellent electrochemical performance as anode materials in supercapacitor. This highlights the low cost and suitable carbon precursor in advanced supercapacitor fabrication.

Also,(Liao et al., 2025) prepare a hierarchically porous carbon was synthesized having high specific surface area, porous and good electrochemical property to store energy. This also reveals that the hemp hurd powder may be used as precursor materials for supercapacitors.

A nanocomposite MOF was synthesized for removal of Pb^{2+} and organic dyes by etching, co-precipitation and carbonization (Cai et al., 2023). This study suggests that MOF are more porous to adsorb the impurities from waste aqueous solutions.

(Munir et al., 2025) demonstrated the way to synthesize ZIF-8/ZIF-67 Composite by solution mixing and self-assembly based method to improve the electrochemical properties for application in supercapacitor applications. As demand for energy production has increased at the current time due to population growth and industrialization. On the other hand, traditional nonrenewable fossil fuel is mainly used as energy sources which leads to release of greenhouse gases responsible for climate change. So, alternative source for fossil fuel is biofuel from various crops as feedstock and Hemp is one of the fastest growing plant on earth and all these studies shows that hemp hurd as an agricultural biproduct suitable for energy storage applications.

2.2 Research Gap

At the early time, the electrochemical properties of carbon are enhanced by the activation method but later on identification of Metal Organic Frameworks (MOF) compound having good crystalline properties and removable porosity were introduced and the researchers are attracted

toward MOF based carbon for the synthesis of high-performance supercapacitor. In the field of energy storage, there is significant research gap to develop structurally stable and highly conductive electrodes. Keeping in mind that there are no any environmental and economic impacts of MOF based hemp hurd carbon, it is selected for the preparation of the Carbon material and study about it. In context of Nepal, there are very few researches that are carried out in the field of energy storage, so this could be one that leads to solve the problem regarding the energy storage and other applications like air purifier, water purifier etc.

2.3 Research Objective

2.3.1 General objective

General objective of the study is to prepare Metal organic Framework based carbon from biowaste material hemp hurd. Such material is characterized by different instrumental techniques and applied for the preparation of supercapacitor.

2.3.2 Specific Objectives

Specific objectives of the study are:

i. Preparation of Hemp hurd based carbon

ii. Preparation of Hemp hurd/Metal Organic Framework based Carbon

iii. Carry out characterization of materials by SEM, EDX and XRD

iv. Electrochemical performance test of materials for supercapacitor

CHAPTER 3: MATERIALS AND METHOD

3.1 Materials Required

Hemp stem were collected from Dadeldhura District of Far Western Province, Nepal.

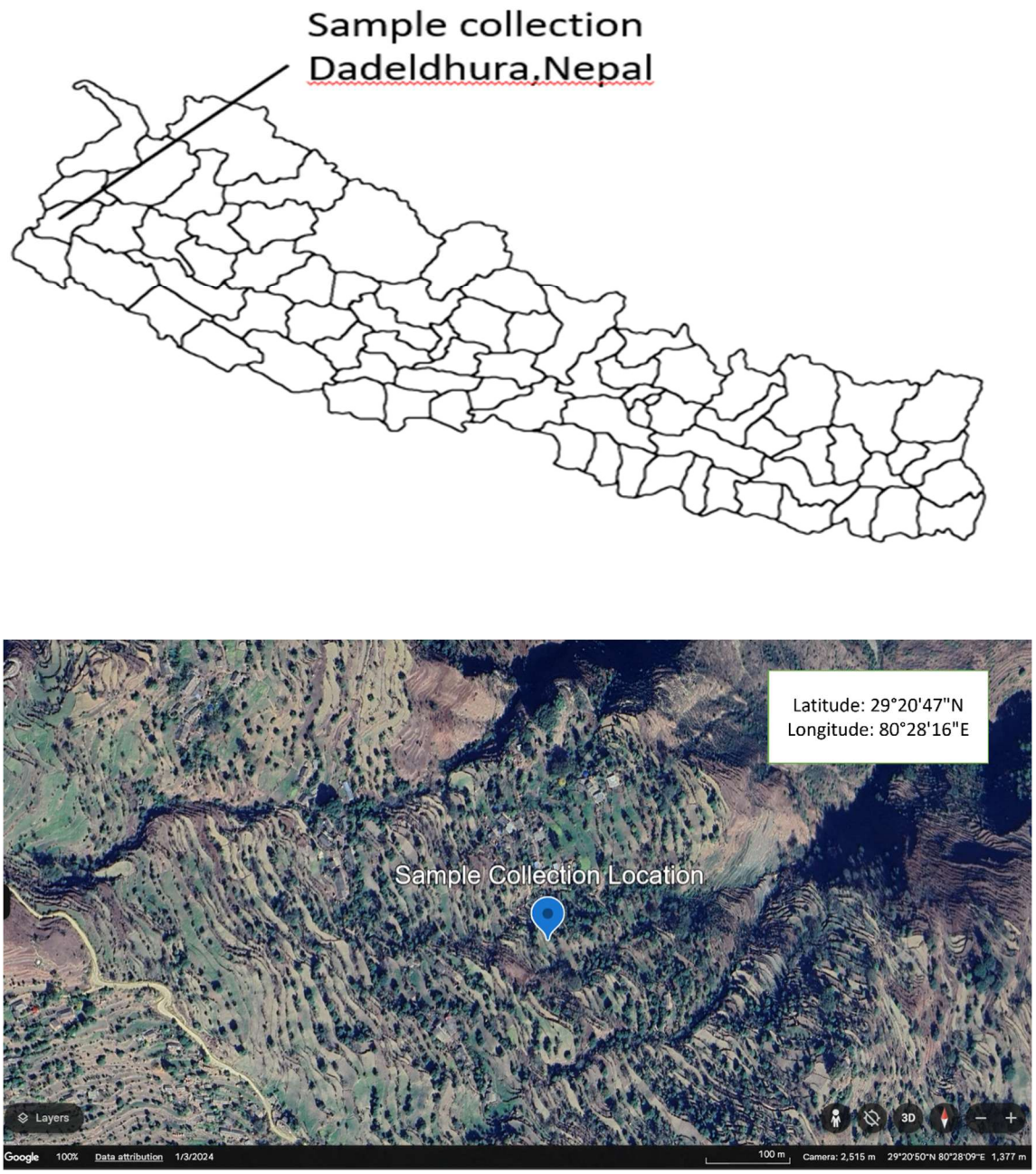

Fig. 5. Map Of Nepal and Sample collected location

3.2 Chemicals

Chemicals that were used for different experiments are listed as below.

i. Cobalt Nitrate hexahydrate (Qualikems, 97% purity)
ii. 2-Methylimidazole (Sigma-Aldrich, 99% purity)
iii. Carbon Black (Loba Chemie)
iv. Potassium Hydroxide (KOH, FIZMERK, India, 85% purity)
v. Iso-propyl alcohol (Central Drug House (P) Ltd., Gujrat, India)
vi. Methanol (Qualigens, 99% purity)
vii. Distilled Water
viii. Ethanol (Changshu Hongsheng Fine Chemical Co. Ltd.)
ix. N_2 Gas
x. Polyvinylidene Difluoride (PVDF)

3.3 Instrument

The instrument used for this study are as tabulated below:

Table 1: Instrument used for experiment

Name of Instrument	Company
Magnetic Stirrer	
weighing balance	Phoenix
Tube Furnace	Keija Furnace "UDIAN"
Sonicator	
Electrochemical Workstation	Corrtest Electrochemical Workstation
Hot Air Oven	Gallenhamp
FSEM and EDX	JBNU CURF EM Lab
XRD	NAST Nepal
FTIR	PerkinElmer spectrometer

3.4 Preparation of Hemp Hurd Powder

The stem of Hemp collected were sun dried for seven days and it was broken into small pieces and consequently ground into fine powder using ball mill. After that fine powder was sieved through standard sieve and dried for 2 days at 60°C.

3.5 Preparation of Metal Organic Framework (MOF)

Sample 1: Methanolic MOF

The Six grams of hemp hurd powder was placed in a beaker. 5.28 grams (0.1512 M) of cobalt nitrate hexahydrate ($Co(NO_3)_2.6H_2O$) was dissolved in 120 mL of methanol to prepare a (0.1512 M) cobalt nitrate solution. The 6-gram sample powder was then mixed with this cobalt nitrate solution and left to shake for a day.

The next day, an imidazole solution was prepared by dissolving 5.91 grams (0.6 M) of 2-methylimidazole in 120 mL of methanol. This imidazole solution was added to the previous mixture containing the sample. The combined solution was stirred gently and then left for another day.

Afterwards, the solution was centrifuged for 10 minutes to separate the components. The supernatant liquid was discarded, and the remaining solid residue was dried at 50°C. This dried residue was collected for further experiments.

Sample 2: MOF Distilled Water

6 g of sample powder was placed in a beaker. 3 g of cobalt nitrate hexahydrate (was dissolved in a mixture of 250 mL distilled water and 50 mL methanol to prepare a (0.0344 M) cobalt nitrate solution. This solution was mixed with the sample powder and left to shake for a day.

In next day, an imidazole solution was prepared by dissolving 2.4 g of imidazole in 120 mL of methanol. This (0.244 M) imidazole solution was added to the previous mixture containing the sample. The combined solution was stirred briefly and then left to sit for another day.

Afterwards, the solution was centrifuged for 10 minutes to separate the components. The supernatant liquid was discarded, and the remaining solid residue was dried at 50°C. The dried residue was collected for further experiments.

Sample 3: MOF Aqueous Cobalt Nitrate and Methanolic Imidazole

6 grams of sample powder was placed in a beaker. 2.5 grams of cobalt nitrate hexahydrate ($Co(NO_3)_2.6H_2O$) was dissolved in 50 mL of Distilled water to prepare a cobalt nitrate solution. The sample powder was then mixed with this (0.178 M) cobalt nitrate solution and left to shake for a day.

In next day, an imidazole solution was prepared by dissolving 0.9 grams of imidazole in 90 mL of methanol. This (0.122 M) imidazole solution was added to the previous mixture containing the sample. The combined solution was stirred briefly and then left to sit for another day.

Afterwards, the solution was collected and 100 mL of methanol was added. Afterwards, the solution was centrifuged for 10 minutes to separate the components The supernatant liquid was discarded, and the remaining solid residue was dried at 50°C. This dried residue was collected for further experiments.

3.6 carbonization of the sample

The samples were weighed using a 4-digit balance, then wrapped in a graphite sheet, and subsequently placed in a tube furnace for carbonization under a nitrogen atmosphere at temperatures: 900 ℃ for 1 h. The temperature ramp rate was set at 5℃ min^{-1} the samples were labeled as in table below:

Table 2: Coding for different Samples

Sample	Sample code
Hemp hurd methanolic MOF carbon carbonized at 900 ℃	HMC 900
Hemp hurd Distilled water MOF carbon carbonized at 900 ℃	HDC 900
Hemp hurd methanolic and Distilled water MOF carbon carbonized at 900 ℃	HDMC 900

Fig. 6. Tube Furnace for Carbonization of samples

3.7 Physiochemical Characterization

The physiochemical characterization of sample was performed by following different characterization techniques:

3.7.1 Fourier Transform Infrared Spectroscopy

Fourier Transform Infrared Spectroscopy (FTIR) is a widely used technique for characterization of materials based on their infrared absorption characteristics and identification of organic and inorganic materials present in that sample (Gong et al., 2024).

In this work, PerkinElmer spectrometer ver. 10.6.2 present in the Department of Chemistry, Amrit Campus, was used for FTIR spectroscopy.

3.7.2 X-Ray Diffraction (XRD)

X-Ray Diffraction (XRD) is a analytical technique applied for analyzing the crystallographic structure, Phase composition and microstructural characteristics of materials.(Akl et al., 2020).

In this work XRD test was performed at Nepal Academy of Science and Technology (NAST), Khumaltar, Lalitpur, Nepal

3.7.3 Scanning Electron Microscopy (SEM)

Scanning Electron Microscopy (SEM) is the powerful imaging technique used for analyzing the surface morphology and microstructural feature of materials by directing focused beam of

electrons onto a specimens surface (Cohen Hyams et al., 2020). In this work SEM analysis was done at Jeonbuk National university, South Korea.

3.7.4 Energy Dispersive Spectroscopy (EDS)

Energy Dispersive Spectroscopy (EDS) also known as Energy Dispersive X-ray Spectroscopy is an analytical technique used to determine the elemental composition of materials (Lin et al., 2023). In this work EDX analysis was done at Jeonbuk National university, South Korea.

3.7.5 Preparation of Working Electrode

For electrochemical measurement, the working electrode was prepared by mixing 80 wt. % prepared sample, 10 wt. % carbon black, and 10 wt. % Polyvinylidene difluoride solutions (8:1:1 ratio) in an agate mortar. The slurry was prepared using isopropyl alcohol as the solvent. The prepared slurry was drop cast in Ni foam (1 cm^2) and dried in an oven at 60 ℃ for 12 hours (Poudel et al., 2021).

3.7.6 Electrochemical Measurement

After the preparation of the electrode, the electrochemical performance of the prepared electrode was measured by using a potentiostat (Corrtest Electrochemical Workstation) using Corrtest CS studio 300 software. Three electrode system was used to perform the electrochemical measurements at room temperature (25 ℃) which consists of the following:

- **Working electrode**: The fabricated electrode was used as the working electrode.
- **Reference electrode**: Ag/AgCl electrode was used as the reference electrode.
- **Counter electrode:** non-reactive and high surface area electrode i.e., Platinum wire was used as the counter electrode.

Electrolyte: 6 M KOH solution was used as the electrolyte.

The three-electrode cell set up is shown in **Fig. 7**

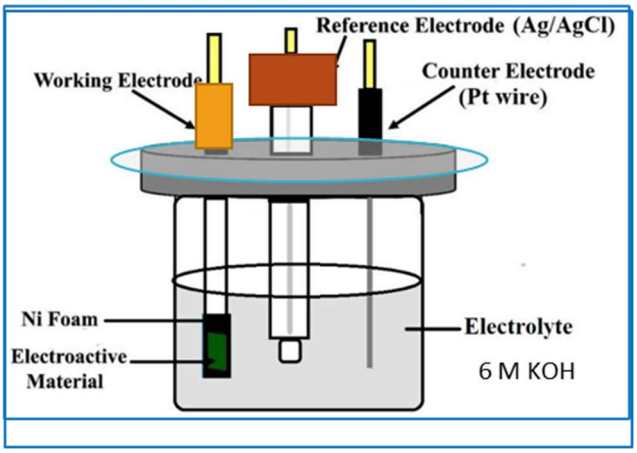

Fig. 7. Three Electrode set up

Fig. 8. Electrochemical Workstation

3.7.7 Cyclic Voltammetry

Cyclic voltammetry is a powerful electrochemical technique employed for investigating how chemical compounds in solution undergo redox reactions. It involves applying a potential to an electrochemical cell and measuring the resulting current. As the potential is swept, the current flowing through the cell is measured. The current arises from the oxidation or reduction of species at the working electrode. the resulting data is typically plotted as current (y-axis) versus applied potential (x-axis). The resulting graph is called a cyclic voltammogram.

In this work, the cyclic voltammetry of the prepared samples was carried out at different scan rates viz. 3, 5, 10, 20, 30, 40, 50, 60, 70, 80, 90, and 100 mV s^{-1} at a potential window of -1 V to 0 V. Peaks identified in the cyclic voltammograms were characterized based on their potential

and current readings. Anodic peaks represented oxidation, while cathodic peaks indicated reduction. The peak current (I_p) and peak potential (E_p) values were determined from the cyclic voltammograms.

3.7.8 Galvanostatic Charge Discharge

Galvanostatic charge discharge (GCD) is a technique utilized in electrochemistry to examine the charging and discharging dynamics of electrochemical cells. In a three- electrode system, charging and discharging processes occur through electrochemical reactions at the working electrode while the potential of the reference electrode remains constant.

In this work, the electrodes were charged and discharged at a constant current density ranging from 1 A g^{-1}, 3 A g^{-1}, 5 A g^{-1}, 7 A g^{-1} and 10 A g^{-1} at the potential window from -1 to 0 V. The voltage-time profiles obtained during the charge-discharge process were analyzed to determine the specific capacitance (C_S) which can be calculated by using following equation.

$$C_s = \frac{\boldsymbol{m} \times \Delta V}{\boldsymbol{i} \times \Delta t}$$

Where:

- Cs = Specific capacitance (F/g)
- i = Discharge current (mA)
- Δt = Discharge time (s)
- ΔV = Voltage window during discharge (V)
- m = Mass of the active material on the electrode (mg)

3.7.9 Electrochemical Impedance Spectroscopy

Electrochemical impedance spectroscopy (EIS) is a powerful technique used in electrochemistry to study the electrical properties of electrochemical systems. In EIS, a small amplitude alternating current (AC) signal is applied to the system over a range of frequencies, typically from millihertz to megahertz. After that, the system's response in terms of voltage and current is examined to learn more about its electrochemical behavior. The impedance of the system, which is the ratio of the applied voltage to the generated current, is measured as a function of frequency. This impedance consists of two components: real (resistive) and imaginary (reactive) components, represented as Z' and - Z'', respectively. Then, impedance

data is plotted on a Nyquist plot (-Z'' vs. Z'). This graph offers significant insights into the system's resistive and capacitive aspects(Shrestha et al., 2019). Through analysis of the Nyquist plot employing equivalent circuit modeling, quantitative details regarding the electrical characteristics of the system, including charge transfer resistance, double-layer capacitance, and solution resistance, can be derived.

In this work, EIS measurements were performed over a frequency range from 1 MHz to 100 KHz at an amplitude of 10 mV. A sinusoidal potential perturbation was applied to the system, and the resulting current response was recorded.

Fig. 9. Schematic Diagram of Preparation of Hemp hurd MOF Carbon

CHAPTER 4: RESULTS AND DISCUSSION

4.1 Carbonization Yield

After the carbonization of the samples, the percentage yield was calculated by using

$$\% \text{ yield} = \frac{\text{Total weight after carbonization}}{\text{Total weight before carbonization}} \times 100 \quad \text{.....(3)}$$

For Different three samples the carbon content was as tabulated below.

Table 3: Carbon content in different three samples

Sample code	Carbonization temperature	Holding time	Weight before Carbonization (g)	Weight after Carbonization (g)	% Yield (%)
HMC 900	900 ℃	1 hr	2.000	0.3545	17.72
HDC 900	900 ℃	1 hr	2.000	0.2885	14.42
HDMC 900	900 ℃	1 hr	4.000	1.030	25.75

From the above data it is seen that the carbon content in the Hemp hurd MOF methanolic carbon (HMC 900) was found to be 17.72%, The carbon content in Hemp hurd distilled water carbon (HDC 900) is 14.42% and the carbon content in Hemp hurd mixed with distilled water and methanol (HDMC 900) was found to be 25.75%. Above three different samples were carbonized at 900℃.

4.2 Fourier Transform Infrared spectroscopy (FTIR)

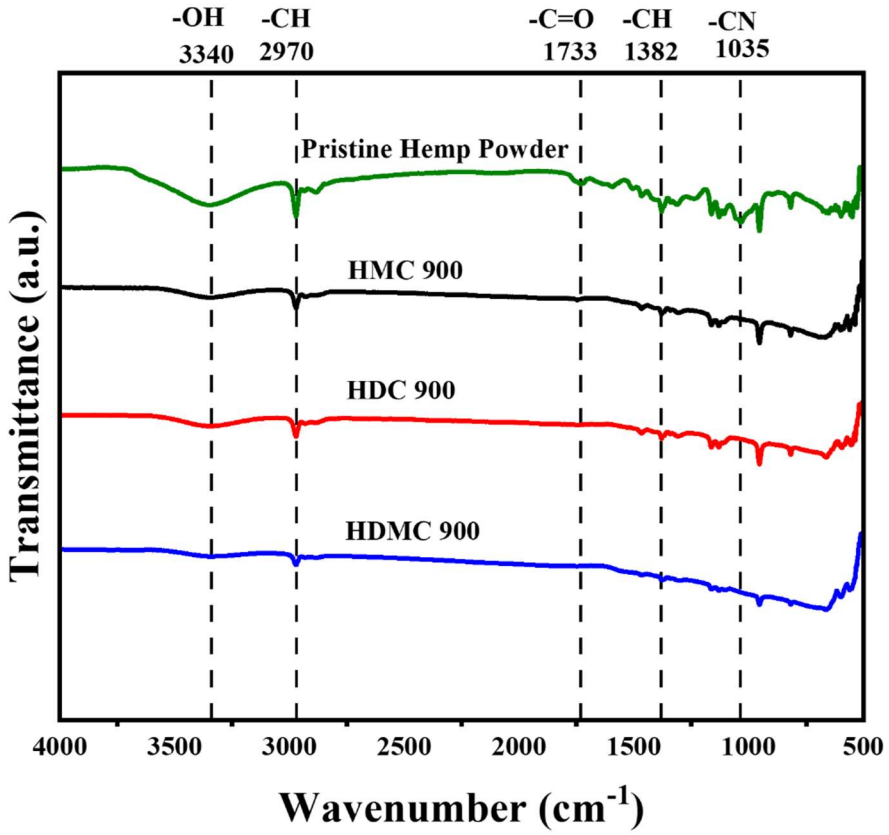

Fig. 10. (a) FTIR Spectra of different sample of Hemp hurd MOF Carbon

Fig. 10 Shows the FTIR spectra of pristine hemp powder before carbonization and others are the Hemp hurd MOF Carbon as stated in graph. The peak appeared at different wavelength shows the different functional group present in the Hemp hurd powder. The broad peak at 3340 cm^{-1} for the Pristine hemp hurd powder corresponds to O-H stretching hydroxyl groups (alcohol). The peak at 2970 cm^{-1} is C-H stretching of the alkane group. The Peak at 1733 cm^{-1} represents the C-O bending aromatic compound whereas the peak at 1382 cm^{-1} shows the C-H bending aldehyde or alkane and 1035 cm^{-1} represents the presence of C-N stretching amine. After carbonization, the major peaks are removed it confirms that the destruction of molecular chain in the aromatic alkene and carbonyl group (Awasthi et al., 2019).

4.3 X-Ray Diffraction (XRD)

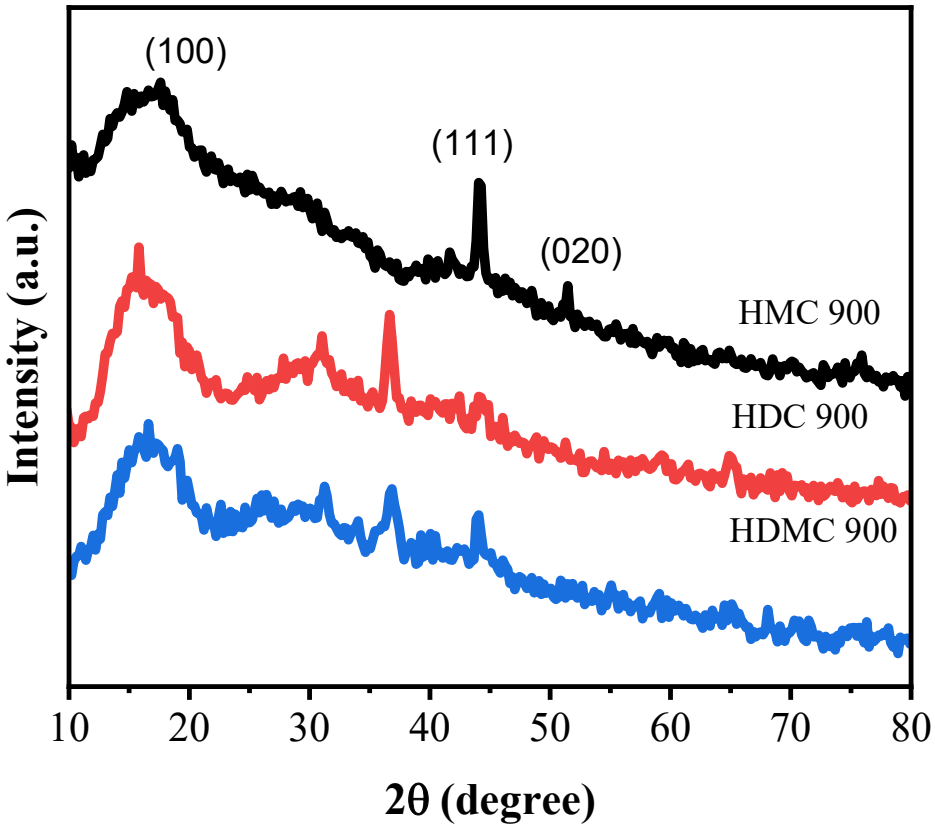

Fig. 11. XRD plot of Different samples of Hemp hurd MOF Carbon

Fig. 11 shows the XRD pattern of the HMC 900, HDC 900 and HDMC 900 which provides valuable information about the sample's composition, crystallinity, and phase purity. Peak around 17° indicates amorphous carbon (100) (X. Liu et al., 2021) and peak at 36 (2θ degree) and 45 (2θ degree) corresponds to the (111), (020) planes for cobalt (Sundriyal et al., 2023). Thus, XRD suggests that there is presence of amorphous carbon and cobalt as crystalline material (Akl et al., 2020). The broad peak suggest that the material is amorphous in nature and sharp peak indicates that the material is crystalline in nature (Wibawa et al., 2020).

4.4 SEM Characterization

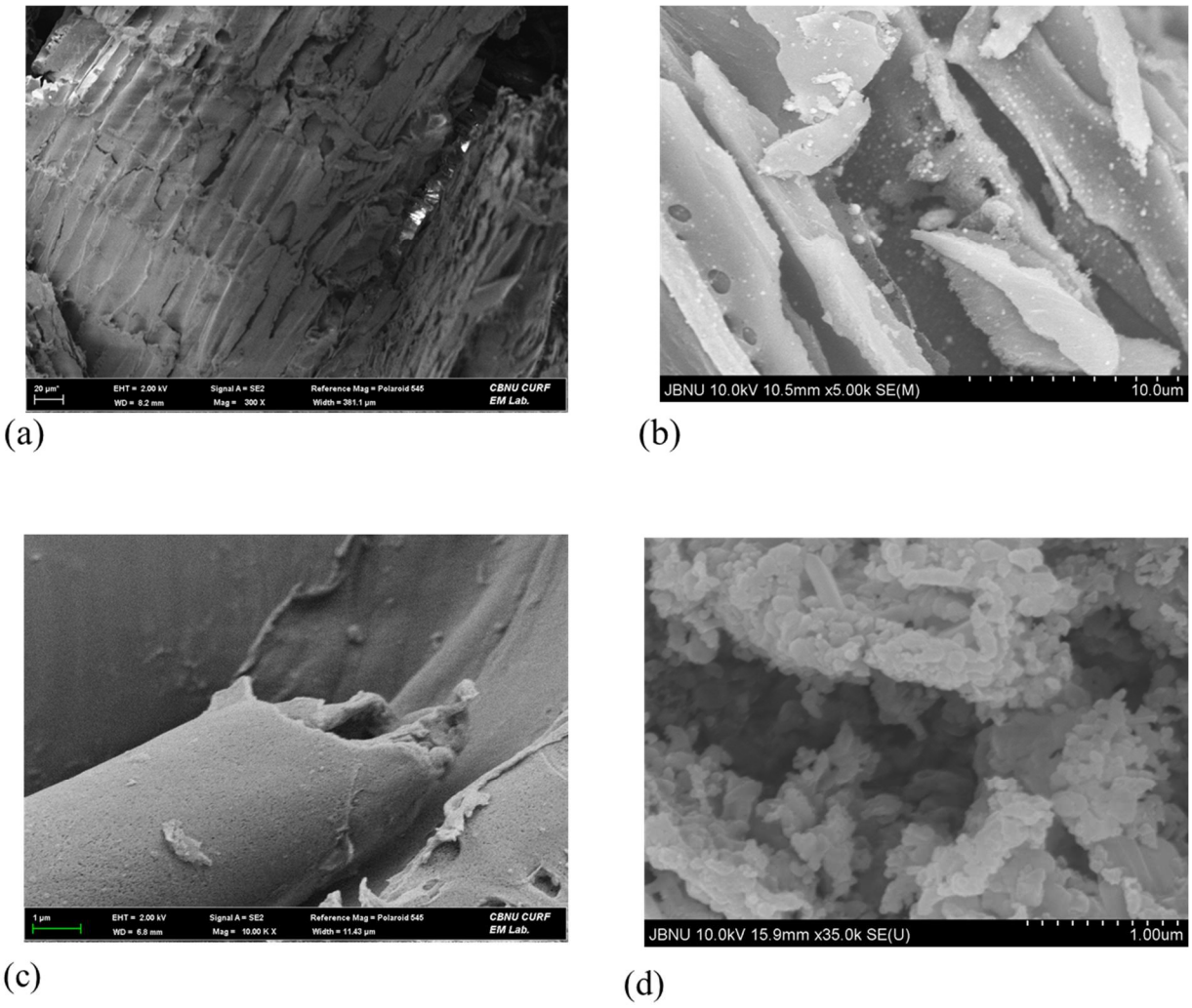

Fig. 12. SEM Image of (a) Pristine Hemp Powder (b) HMC 900 (C)HDC 900 and (d)HDMC 900

Shows the SEM image of (a) Pristine hemp powder (b) HMC 900 (c) HDC 900 and (d) HDMC 900 respectively**. Fig. 12** (a) suggests that there are small pores in the pristine sample and the atomic particles are attached with each other. Similarly, the SEM image of MOF carbon sample suggest that there is the porous structure (Bullock et al., 2025).

4.5 Electron Dispersive X-ray spectroscopy (EDX)

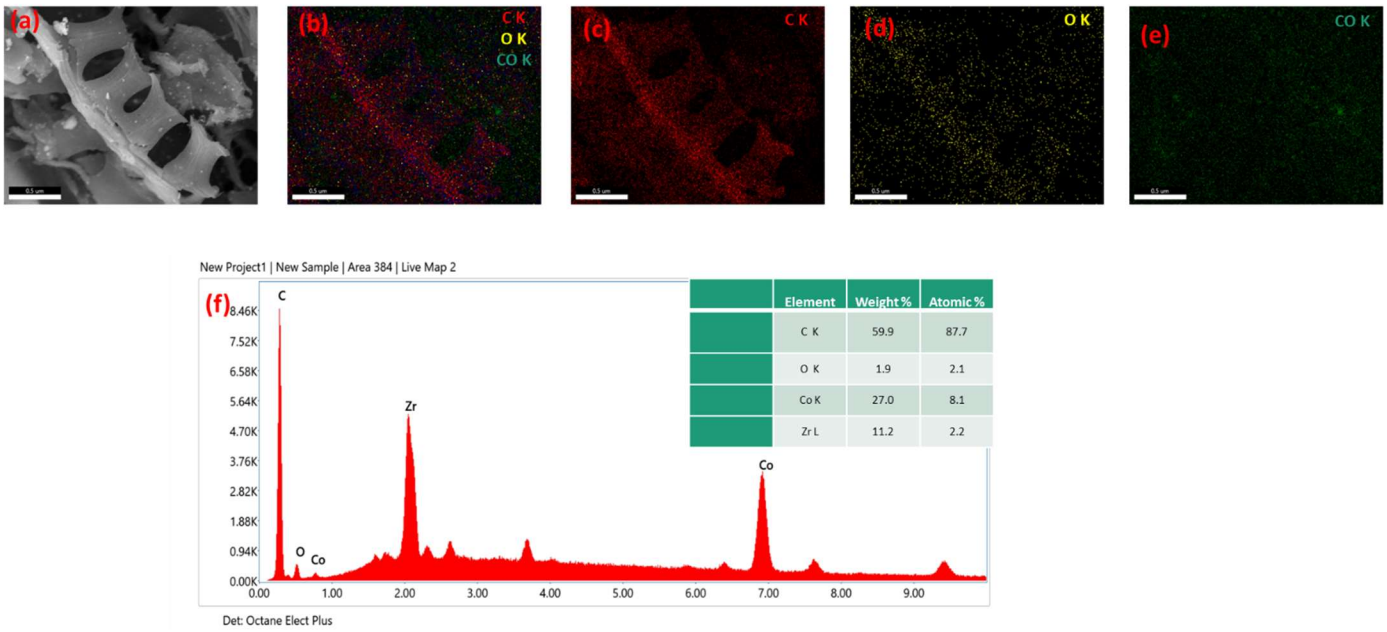

Fig. 13. *(a)SEM Image of Hemp hurd MOF carbon (b)* Elemental mapping of HMC 900 (c)Carbon (d) Oxygen (e) Cobalt (f) EDX spectrum for Hemp hurd MOF carbon

Fig. 13. Represents the Energy Dispersive X-ray Spectroscopy (EDS or EDX) spectrum used to analyze the elemental composition of Hemp hurd MOF. X-axis represents the energy of detected X-rays and Y-axis represents the intensity of X-ray detected at each energy level. Different peak in the graph represents the specific element in sample. The first peak in the graph shows the presence of Carbon with weight percentage of 59,9% and an atomic percentage of 87.7%. Similarly smaller peak just after Carbon shows the presence of Oxygen and Cobalt with weight percentage of 1.9% & 27% and Atomic Percentage of 2.1% & 8.1% respectively. According to the quantitative data, Cobalt id the second most abundant element by weight (27%). Zirconium is shown in the peak due to misidentification of instrument of overlapping energy levels close to that of it (Aryal et al., 2025).

4.6 Electrochemical measurement

Electrochemical measurement of the fabricated electrode s i.e., HMC 900, HDC 900 and HDMC 900 were carried out using three-electrode system with Ag/AgCl as reference electrode and Platinum wire as a counter electrode in 6M KOH solution at room temperature in the potential range of -1.0 to 0 V

4.6.1 Cyclic Voltammetry (CV)

The Cyclic Voltammetry experiment was carried out in the potential range of -1 to 0 V for all three samples HMC 900, HDC 900 and HDMC 900 at various scan rates viz. 5, 10, 20, 30, 40, 50 and 60 mVs^{-1} are shown in **Fig. 14, Fig. 15 and Fig. 16** respectively.

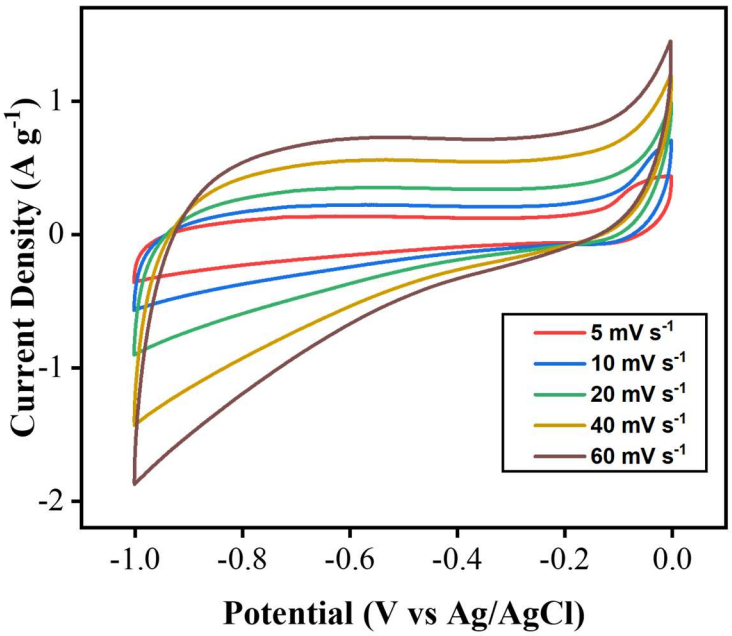

Fig. 14. CV plot of HMC 900 at different scan rates

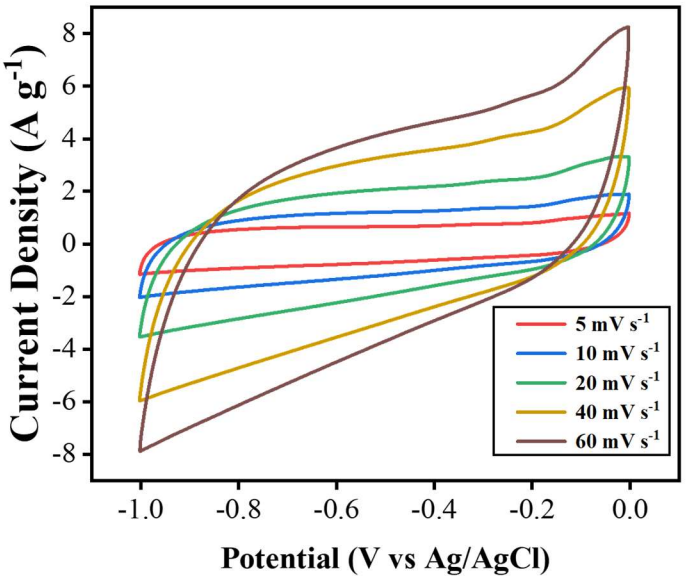

Fig. 15. CV plot of HDC 900 at different scan rates

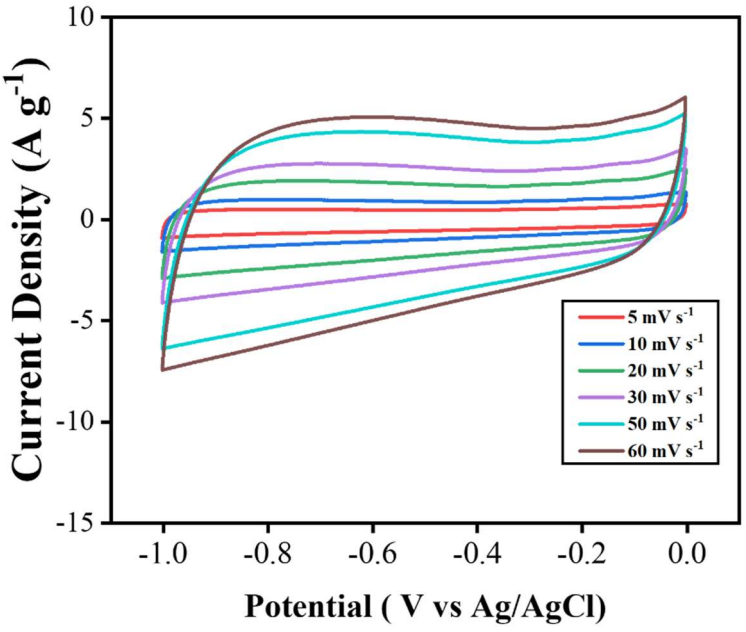

Fig. 16. CV plot of HDMC 900 at different scan rates

The Cyclic Voltammetry (CV) curve of three different sample shows the quasi-rectangular shape at different scan rates ranging from 5 to 60 mVs^{-1}, this also indicates the electrochemical double layer

capacitance (EDLC) behavior. The absence of distinct redox peaks assure that the charge storage mechanism is primarily non faradaic and was due to ion adsorption and desorption at electrode-electrolyte interface. At lower scan rates, the CV curve is more rectangular due to better ion diffusion throughout the porous carbon matrix. As scan rate increases, there is slight distortion in curve which is due to kinetic limitation in ion transport within micropores. All these characteristics suggests that the material will be viable and sustainable for energy storage (Men et al., 2021).

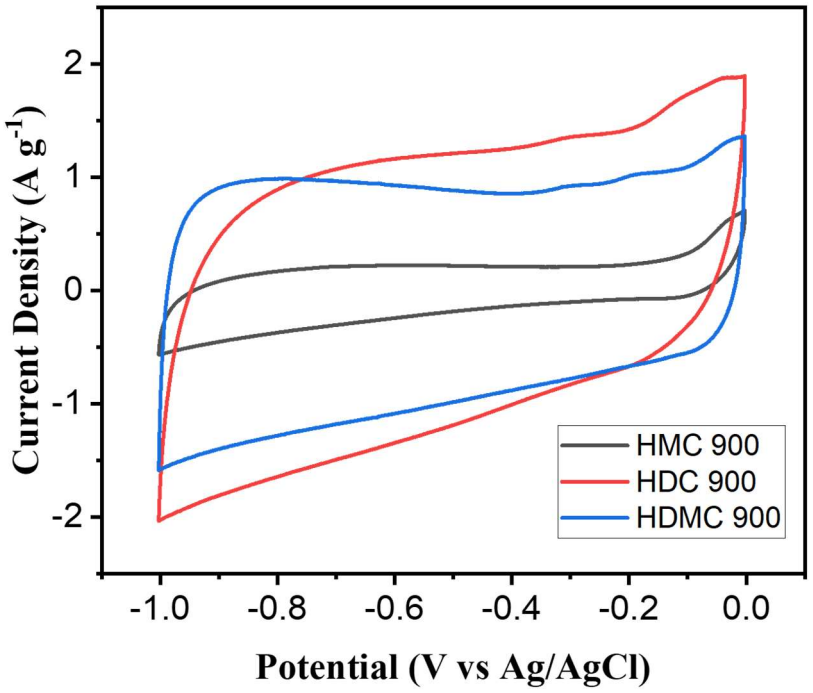

Fig. 17. Comparison of CV curves of HMC 900, HDC 900 at scan rate 10 mVs^{-1}

Among three different samples HMC 900, HDC 900 and HDMC 900, the CV plot of HDMC 900 shows more integrated area under the curve and rectangular shape indicating superior electrochemical double layer capacitance (EDLC) performance. Similarly, CV plot of HDC 900 also shows that it has great performance in EDLC performance but the CV plot of HMC shows that HMC 900 has weaker capacitive behavior.

4.6.2 Galvanostatic Charge Discharge (GCD)

The GCD plot of HMC 900, HDC 900 and HDMC 900 at different current densities from 1 to 10 Ag^{-1} under the basic electrolyte 6M KOH within the system are shown in **Fig.**. The specific capacitance (Fg^{-1}) of different electrode material was calculated from Galvanometric Charge Discharge (GCD) curve using following equation.

$$C = \frac{I \times \Delta t}{m \times \Delta v} \qquad (1)$$

Where I = the charge discharge Current (mA),

Δt = discharge time (s),

m = the active mass of the sample deposited on Nickel foam (mg)

and Δv = the potential (v).

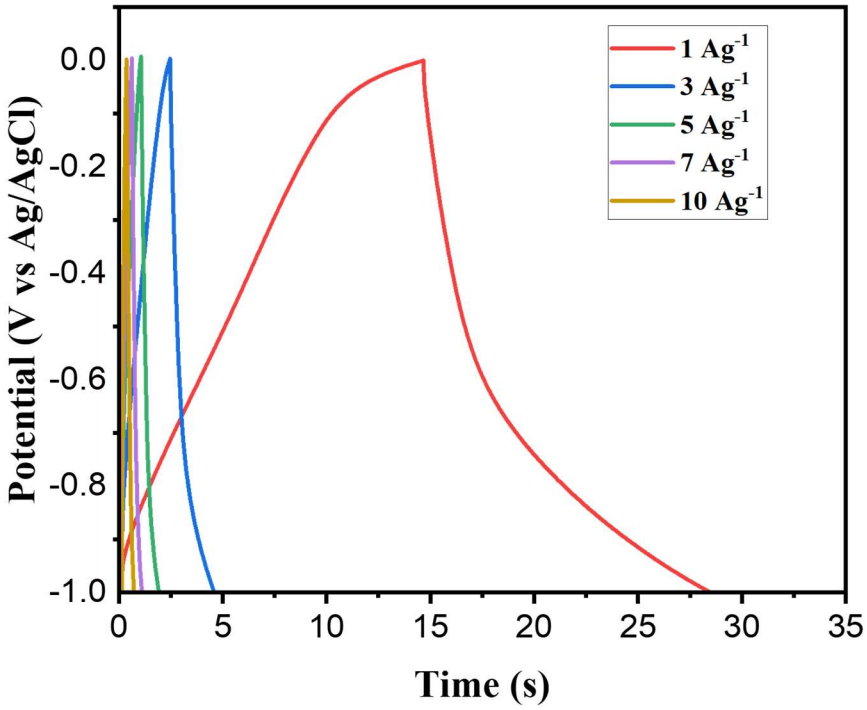

Fig. 18. GCD plot of HMC 900 at different current densities

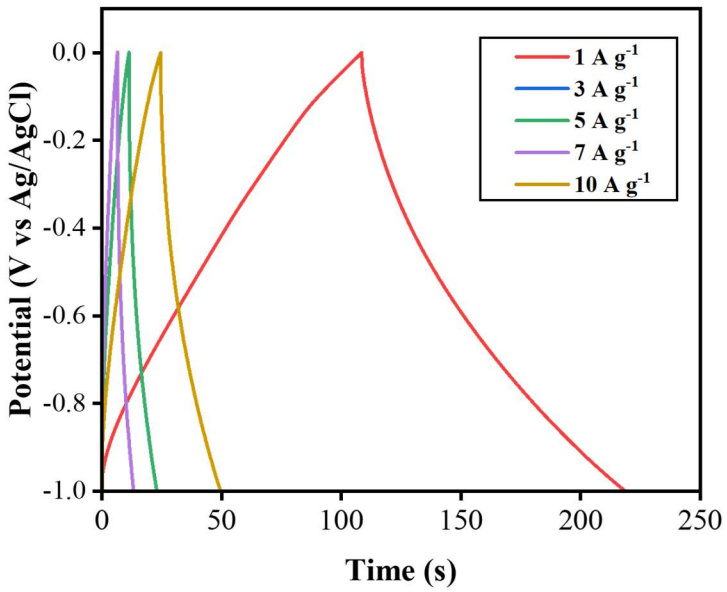

Fig. 19. GCD plot of HDC 900 at different current densities

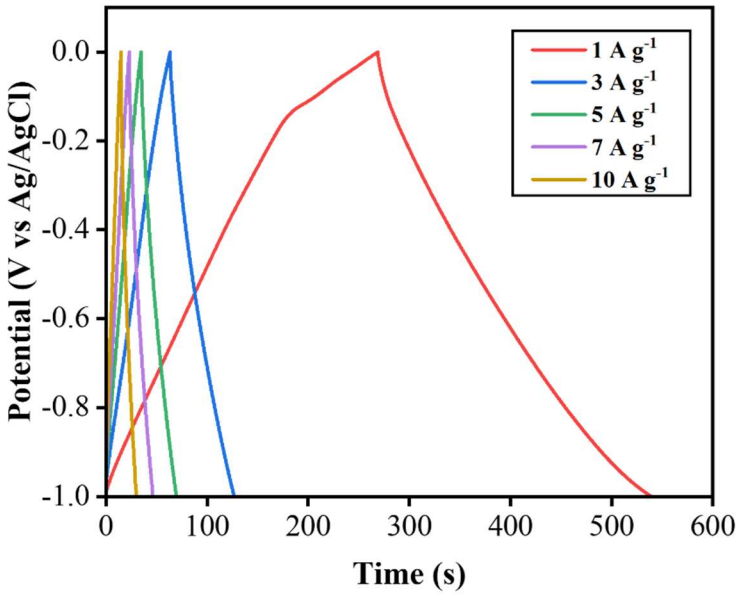

Fig. 20. GCD plot of HDMC 900 at different current densities

Fig. 18, Fig. 19 & Fig. 20 represents the Galvanometric Charge discharge (GCD) curve of different sample HMC 900, HDC 900 and HDMC 900 respectively at different current densities

as shown in graph. The linear GCD plot indicates that the carbon is easily penetrated in electrode i.e., Nickel form. HMC 900 shows the specific capacitance of 13.83, 6.40, 4.30, 3.45 and 3.30 Fg^{-1} at current densities of 1,3,5,7 and 10 Ag^{-1} respectively. Similarly, HDC 900 GCD plot shows the Specific capacitance of 110.10, 75.12, 58.19, 47.18 and 41 Fg^{-1} at current densities of 1,3,5,7 and 10 Ag^{-1} respectively and The HDMC 900 shows the specific capacitance of 270.47, 190.08, 174.65,163.59 and 151.40 Fg^{-1} at current densities of 1,3,5,7 and 10 Ag^{-1} respectively. The highest specific capacitance and longer discharge time are obtained in Hemp hurd distilled water and methanolic MOF (HDMC 900) which indicates that the mix MOF is best among all samples for further applications.

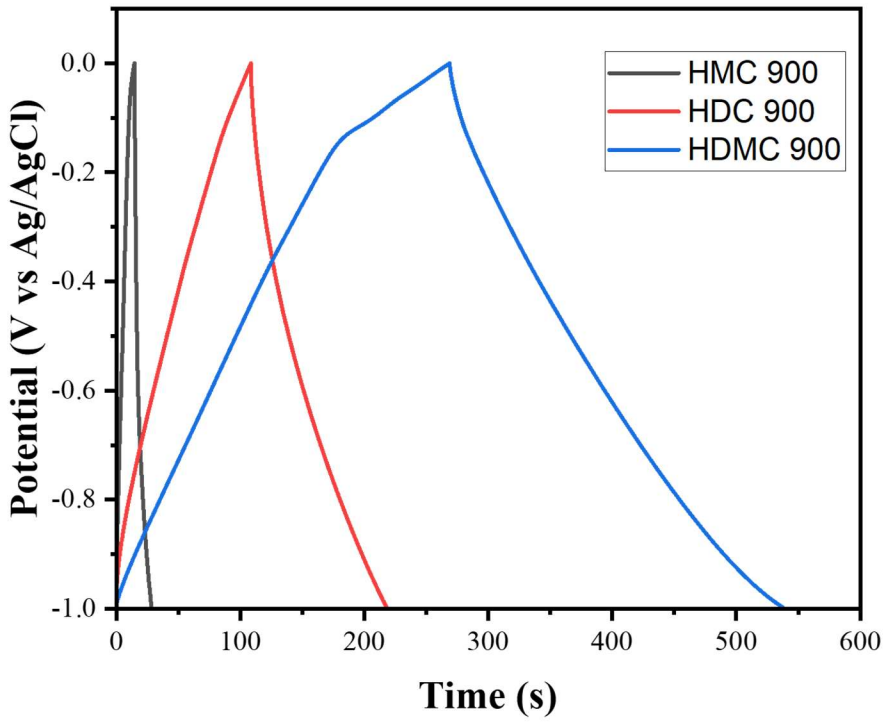

Fig. 21. Comparison of GCD plot of HMC 900, HDC 900 and HDMC 900 electrodes at current density of 1 Ag^{-1}

Fig. 21 Shows the comparison of GCD curve of HMC 900, HDC 900 and HDMC 900 at current density of 1 Ag^{-1}. This Curve shows that the charging and discharging time of HMC 900 was least, for HDC 900 the charging and discharging time was moderate and the charging and

discharging time for HDMC 900 was highest. If the discharge time is more, then it has higher specific capacitance and greater efficiency for super capacitor application.

The Comparative representation of specific capacitance vs current density of HMC 900, HDC 900 and HDMC 900 is shown in **Fig.21.** and the specific capacitance found at current density of 1 Ag^{-1} were tabulated as below.

Table 4: Comparison of specific capacitance of different samples

Current density (A g^{-1})	Specific Capacitance (Fg^{-1})		
	HMC 900	HDC 900	HDMC 900
1	13.83	110.10	270.47

Comparing the Specific capacitance value with (Minakshi et al., 2024), The specific capacitance of activated carbon of hemp stalk by chemical activation with potassium hydroxide(KOH) was 240 Fg^{-1} and in this study it was found that in HDMC 900 the specific capacitance was 270.47 Fg^{-1}. Since, MOF increases the porosity and metallic ions present adds ionic conductivity to sample. So, higher value of specific capacitance was obtained.

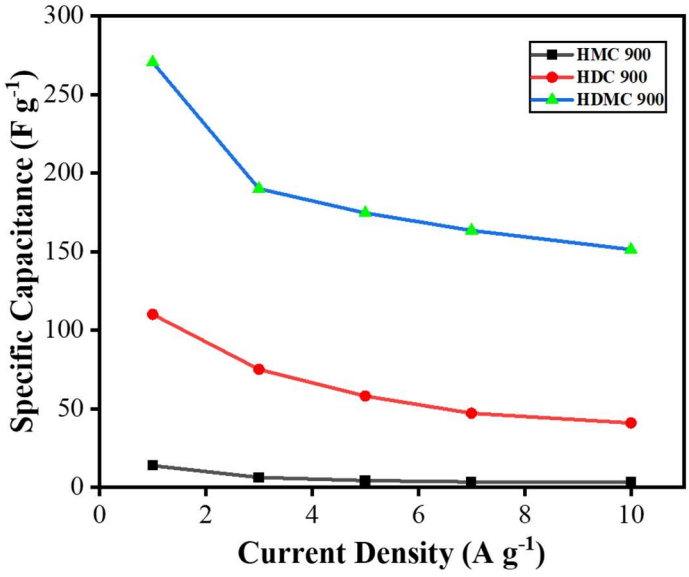

Fig. 22. Specific Capacitance vs Current density plot of different three samples

The graph of Specific capacitance (Fg^{-1}) versus current density (Ag^{-1}) for three samples, namely HMC 900, HDC 900, and HDMC 900, is shown in **Fig. 22**. The capacitance decreases with increasing current density for the three samples. Among them, HDMC 900 has the best specific capacitance at every current density, starting from about 270 Fg^{-1} at 1 Ag^{-1} and reducing steadily to about 151.4 Fg^{-1} at 10 Ag^{-1}. HDC 900's performance is midrange, beginning at about 110.10 Fg^{-1} and dropping to about 41 Fg^{-1} at the highest current density. HMC 900 performs worst of all at all current densities, never exceeding 13.83 Fg^{-1}. This trend shows that HDMC 900 has superior electrochemical performance, likely due to a more favorable structure or composition for charge storage. The data shows the effectiveness of the HDMC 900 material in retaining higher capacitance even when subjected to greater current loads.

4.6.3 Electrochemical Impedance Spectroscopy (EIS)

EIS measurements were performed over a frequency range from 1 MHz to 100 KHz at an amplitude of 10 mV. A sinusoidal potential perturbation was applied to the system, and the resulting current response was recorded. Then, impedance data was plotted on a Nyquist plot (-Z'' vs. Z') which is shown in graph below.

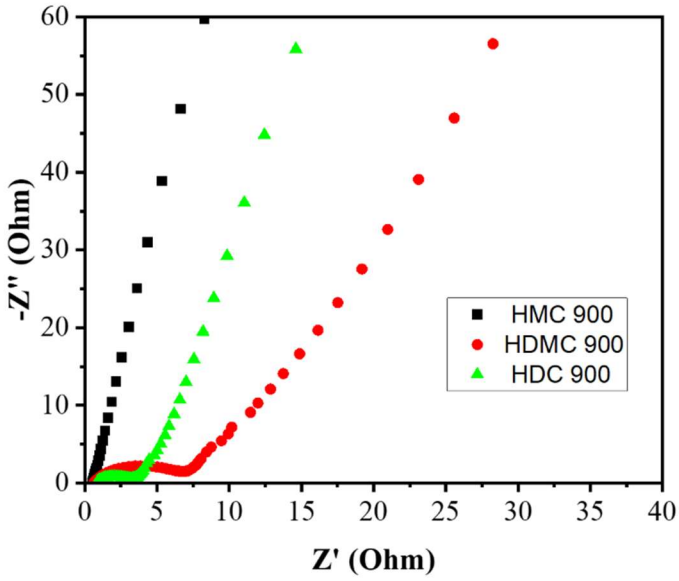

Fig. 23. Electrochemical Impedance Curve Different Sample of Hemp hurd MOF Carbon

The combined Nyquist plot for EIS results was drawn for HMC 900, HDC 900 and HDMC 900 which is shown in **Fig. 23.**

CHAPTER 5: CONCLUSIONS AND RECOMMENDATIONS

5.1 Conclusion

In conclusion, Sample preparation of Hemp hurd MOF from Cobalt nitrate and 2-methylimidazole was done and Carbonization was performed under a Nitrogen atmosphere at temperatures 900 ℃ for 1 h. The temperature ramp rate was set at 5℃ min^{-1}. Different electrochemical tests were done and Metal-Organic Framework (MOF) modification of Hemp hurd carbon was investigated for supercapacitor applications. By increasing surface area and creating linked porous channels that are advantageous for ion transport, the structural and morphological investigation conducted. Using Scanning Electron Microscopy (SEM) verified the successful integration of MOF onto the porous hemp hurd carbon framework. The existence of functional groups linked to MOF was further confirmed by Fourier Transform Infrared Spectroscopy (FTIR) analysis. Cyclic Voltammetry (CV), Galvanostatic Charge Discharge (GCD) and Electrochemical Impedance Spectroscopy (EIS) test were used to assess the electrochemical performance. Due to the MOF-modified surface, the CV curves showed a nearly rectangular form, which suggests EDLC type supercapacitor behavior with improved charge storage capabilities. The Specific Capacitance is 13.83, 110.10 and 270.47 F g^{-1} for HMC 900, HDC 900 and HDMC 900 respectively. EDX suggested that the abundant element is carbon with weight percentage of 59.9% and atomic percentage of 87.7%. XRD shows that the carbon formed was amorphous as well as presence of sharp peak suggests the crystalline nature due to presence of Cobalt.

5.2 Recommendations

- Conduct more detailed studies on the porosity and surface area using BET (Brunauer-Emmett-Teller) analysis.
- Use advanced imaging techniques like high-resolution transmission electron microscopy (HRTEM) to gain deeper insights into the pore structure and distribution.
- Develop methods for scaling up the synthesis process while maintaining consistent quality and performance of the carbon materials.
- Integrate the prepared materials into prototype supercapacitor devices.
- Perform computational studies to understand the charge storage mechanisms at the atomic and molecular levels, providing insights that can guide further material design and optimization.

REFERENCES

Akl, A. A., El Radaf, I. M., & Hassanien, A. S. (2020). Intensive comparative study using X-Ray diffraction for investigating microstructural parameters and crystal defects of the novel nanostructural ZnGa2S4 thin films. *Superlattices and Microstructures*, *143*, 106544. https://doi.org/https://doi.org/10.1016/j.spmi.2020.106544

Aryal, S., Shrestha, K. R., Shrestha, T., Oli, H. B., Pathak, I., Shrestha, R. L., & Bhattarai, D. P. (2025). Activated carbon from Prunus persica seed stones as a negatrode material for high-performance supercapacitors. *Journal of Molecular Structure*, *1323*, 140810. https://doi.org/https://doi.org/10.1016/j.molstruc.2024.140810

Awasthi, G. P., Bhattarai, D. P., Maharjan, B., Kim, K.-S., Park, C. H., & Kim, C. S. (2019). Synthesis and characterizations of activated carbon from Wisteria sinensis seeds biomass for energy storage applications. *Journal of Industrial and Engineering Chemistry*, *72*, 265-272.

Bullock, E. S., von der Handt, A., & Halfpenny, A. (2025). Scanning electron microscopy, electron probe microanalysis, and electron backscatter diffraction in the geological sciences. In A. Anbar & D. Weis (Eds.), *Treatise on Geochemistry (Third edition)* (pp. 789-828). Elsevier. https://doi.org/https://doi.org/10.1016/B978-0-323-99762-1.00087-5

Cai, H., Ma, K., Zhang, Y., Li, X., Wang, W., & Tong, S. (2023). Carbonizing hollow metal–organic framework/layered double hydroxide (MOF/LDH) nanocomposite with excellent adsorption capacity for removal of Pb(II) and organic dyes from wastewater. *Carbon Research*, *2*(1), 23. https://doi.org/10.1007/s44246-023-00058-0

Cevher, D., & Çırpan, A. (2025). Design, strategies and recent advances in conjugated polymers for supercapacitors. *Journal of Energy Storage*. https://doi.org/10.1016/j.est.2024.115246

Chhetri, K., Tiwari, A. P., Dahal, B., Ojha, G. P., Mukhiya, T., Lee, M., Kim, T., Chae, S.-H., Muthurasu, A., & Kim, H. Y. (2020). A ZIF-8-derived nanoporous carbon nanocomposite wrapped with Co3O4-polyaniline as an efficient electrode material for an asymmetric supercapacitor. *Journal of Electroanalytical Chemistry*, *856*, 113670. https://doi.org/https://doi.org/10.1016/j.jelechem.2019.113670

Choudhary, N., Li, C., Moore, J., Nagaiah, N., Zhai, L., Jung, Y., & Thomas, J. (2017). Asymmetric Supercapacitor Electrodes and Devices. *Advanced Materials*, *29*. https://doi.org/10.1002/adma.201605336

Cohen Hyams, T., Mam, K., & Killingsworth, M. C. (2020). Scanning electron microscopy as a new tool for diagnostic pathology and cell biology. *Micron*, *130*, 102797. https://doi.org/https://doi.org/10.1016/j.micron.2019.102797

Gamby, J., Taberna, P. L., Simon, P., Fauvarque, J. F., & Chesneau, M. (2001). Studies and characterisations of various activated carbons used for carbon/carbon supercapacitors. *Journal of Power Sources*, *101*(1), 109-116. https://doi.org/https://doi.org/10.1016/S0378-7753(01)00707-8

Gao, Y., Yue, Q., Gao, B., & Li, A. (2020). Insight into activated carbon from different kinds of chemical activating agents: A review. *Science of The Total Environment*, *746*, 141094. https://doi.org/https://doi.org/10.1016/j.scitotenv.2020.141094

Gong, Y., Chen, X., & Wu, W. (2024). Application of fourier transform infrared (FTIR) spectroscopy in sample preparation: Material characterization and mechanism investigation. *Advances in Sample Preparation*, *11*, 100122. https://doi.org/https://doi.org/10.1016/j.sampre.2024.100122

Guo, H., Zhang, J., Xu, M., Wang, M., Yang, F., Wu, N., Zhang, T., Sun, L., & Yang, W. (2021). Zeolite-imidazole framework derived nickel-cobalt hydroxide on ultrathin MXene nanosheets for long life and high performance supercapacitance. *Journal of Alloys and Compounds*, *888*, 161250. https://doi.org/https://doi.org/10.1016/j.jallcom.2021.161250

Hançer Güleryüz, E., & Özen, D. N. (2022). Advanced exergy and exergo-economic analyses of an advanced adiabatic compressed air energy storage system. *Journal of Energy Storage*, *55*, 105845. https://doi.org/https://doi.org/10.1016/j.est.2022.105845

He, X., & Zhang, X. (2022). A comprehensive review of supercapacitors: Properties, electrodes, electrolytes and thermal management systems based on phase change materials. *Journal of Energy Storage*, *56*, 106023. https://doi.org/https://doi.org/10.1016/j.est.2022.106023

Hu, Q., Yang, R., Mo, Z., Lu, D., Yang, L., He, Z., Zhu, H., Tang, Z., & Gui, X. (2019). Nitrogen-doped and Fe-filled CNTs/NiCo2O4 porous sponge with tunable microwave absorption performance. *Carbon*, *153*, 737-744. https://doi.org/https://doi.org/10.1016/j.carbon.2019.07.077

Kumar, N., Kim, S.-B., Lee, S., & Park, S. J. (2022). Recent Advanced Supercapacitor: A Review of Storage Mechanisms, Electrode Materials, Modification, and Perspectives. *Nanomaterials*, *12*. https://doi.org/10.3390/nano12203708

Liao, Q., Wan, S., Liu, Y., Niu, X., Zhang, D., Li, H., & Wang, K. (2025). Hemp-derived hierarchically porous carbon cathode enabling high energy storage for advanced zinc-ion hybrid capacitor. *Journal of Energy Storage*, *115*, 115975. https://doi.org/https://doi.org/10.1016/j.est.2025.115975

Libich, J., Máca, J., Vondrák, J., Čech, O., & Sedlaříková, M. (2018). Supercapacitors: Properties and applications. *Journal of Energy Storage*, *17*, 224-227. https://doi.org/https://doi.org/10.1016/j.est.2018.03.012

Lin, W. M., Yoshida, T., Suresh, G., Pradeepkumar Gupta, V., Ozeki, S., Oyama, K., Akiyama, T., Yaakob, Y., Asaka, T., Yong, Y., Miyazaki, H., Sonoyama, N., & Tanemura, M. (2023). Controllable fabrication of Au-nanoprotrusion arrays as a platform for the materials design and characterization. *Applied Surface Science*, *613*, 156011. https://doi.org/https://doi.org/10.1016/j.apsusc.2022.156011

Liu, R., Zhou, A., Zhang, X., Mu, J., Che, H., Wang, Y., Wang, T., Zhang, Z., & Kou, Z. (2021). Fundamentals, advances and challenges of transition metal compounds-based supercapacitors. *Chemical Engineering Journal*, *412*, 128611. https://doi.org/10.1016/J.CEJ.2021.128611

Liu, X., Ma, Y., Cai, Y., Hu, S., Chen, J., Liu, Z., & Wang, Z. (2021). Zeolitic imidazole framework derived N-doped porous carbon/metal cobalt nanoparticles hybrid for oxygen electrocatalysis and rechargeable Zn–air batteries [10.1039/D1RA01350E]. *RSC Advances*, *11*(26), 15722-15728. https://doi.org/10.1039/D1RA01350E

Liu, X., Xue, F., & Adhikari, B. (2024). Recent advances in plant protein modification: spotlight on hemp protein. *Sustainable Food Technology*, *2*(4), 893-907. https://doi.org/https://doi.org/10.1039/d3fb00215b

Men, S., Zheng, H., Ma, D., Huang, X., & Kang, X. (2021). Unraveling the stabilization mechanism of solid electrolyte interface on ZnSe by rGO in sodium ion battery. *Journal of Energy Chemistry*, *54*, 124-130. https://doi.org/https://doi.org/10.1016/j.jechem.2020.05.046

Minakshi, M., Mujeeb, A., Whale, J., Evans, R., Aughterson, R., Shinde, P. A., Ariga, K., & Shrestha, L. K. (2024). Synthesis of Porous Carbon Honeycomb Structures Derived from Hemp for Hybrid Supercapacitors with Improved Electrochemistry. *ChemPlusChem*, *89*(12), e202400408. https://doi.org/https://doi.org/10.1002/cplu.202400408

Mukhiya, T., Muthurasu, A., Tiwari, A. P., Chhetri, K., Chae, S.-H., Kim, H., Dahal, B., Lee, B. M., & Kim, H. Y. (2021). Integrating the Essence of a Metal–Organic Framework with

Electrospinning: A New Approach for Making a Metal Nanoparticle Confined N-Doped Carbon Nanotubes/Porous Carbon Nanofibrous Membrane for Energy Storage and Conversion. *ACS Applied Materials & Interfaces*, *13*(20), 23732-23742. https://doi.org/10.1021/acsami.1c04104

Munir, O., Saleem, M., Manzoor, M. Z., Shahzad, A., Shahid, S., Arif, S. M. B., & Akhtar, M. N. (2025). Novel ZIF-8/ZIF-67 and multi-wall carbon nanotubes ternary composite: A promising electrode material for high capacitance supercapacitors. *Materials Chemistry and Physics*, *338*, 130672. https://doi.org/https://doi.org/10.1016/j.matchemphys.2025.130672

Norouzbahari, S., Mehri Lighvan, Z., Ghadimi, A., & Sadatnia, B. (2023). ZIF-8@Zn-MOF-74 core–shell metal–organic framework (MOF) with open metal sites: Synthesis, characterization, and gas adsorption performance. *Fuel*, *339*, 127463. https://doi.org/https://doi.org/10.1016/j.fuel.2023.127463

Park, Y.-k., Park, G.-g., Park, J.-g., & Lee, J.-w. (2017). Robust Free-standing Electrodes for Flexible Lithium-ion Batteries Prepared by a Conventional Electrode Fabrication Process. *Electrochimica Acta*, *247*, 371-380. https://doi.org/https://doi.org/10.1016/j.electacta.2017.07.032

Poudel, M. B., Shin, M., & Kim, H. J. (2021). Polyaniline-silver-manganese dioxide nanorod ternary composite for asymmetric supercapacitor with remarkable electrochemical performance. *International Journal of Hydrogen Energy*, *46*(1), 474-485. https://doi.org/https://doi.org/10.1016/j.ijhydene.2020.09.213

Pullas Navarrete, J., & de la Torre, E. (2022). Preparation of activated carbon fibers (ACF) impregnated with metallic silver particles from cotton-woven wastes and its performance as an antibacterial agent. *Materials Today Communications*, *33*, 104598. https://doi.org/https://doi.org/10.1016/j.mtcomm.2022.104598

Raoof, J. B., Hosseini, S. R., Ojani, R., & Mandegarzad, S. (2015). MOF-derived Cu/nanoporous carbon composite and its application for electro-catalysis of hydrogen evolution reaction. *Energy*, *90*. https://doi.org/10.1016/j.energy.2015.08.013

Rosas, J. M., Bedia, J., Rodríguez-Mirasol, J., & Cordero, T. (2009). HEMP-derived activated carbon fibers by chemical activation with phosphoric acid. *Fuel*, *88*(1), 19-26. https://doi.org/https://doi.org/10.1016/j.fuel.2008.08.004

Şahin, M. E., Blaabjerg, F., & Sangwongwanich, A. (2022). A Comprehensive Review on Supercapacitor Applications and Developments. *Energies*, *15*(3), 674. https://www.mdpi.com/1996-1073/15/3/674

Shrestha, D., Maensiri, S., Wongpratat, U., Lee, S. W., & Nyachhyon, A. R. (2019). Shorea robusta derived activated carbon decorated with manganese dioxide hybrid composite for improved capacitive behaviors. *Journal of Environmental Chemical Engineering*, *7*(5), 103227. https://doi.org/https://doi.org/10.1016/j.jece.2019.103227

Simon, P., & Gogotsi, Y. (2008). Materials for electrochemical capacitors. *Nature Materials*, *7*(11), 845-854. https://doi.org/10.1038/nmat2297

Srinivasan, R., Elaiyappillai, E., Nixon, E. J., Sharmila Lydia, I., & Johnson, P. M. (2020). Enhanced electrochemical behaviour of Co-MOF/PANI composite electrode for supercapacitors. *Inorganica Chimica Acta*, *502*, 119393. https://doi.org/https://doi.org/10.1016/j.ica.2019.119393

Sundriyal, S., Dubey, P., Mansi, Gupta, B., Holdynski, M., Bonarowska, M., Deep, A., Shrivastav, V., & Nogala, W. (2023). Zeolitic Imidazole Framework Derived Cobalt Phosphide/Carbon Composite and Waste Paper Derived Porous Carbon for High-Performance Supercapattery. *Advanced Materials Interfaces*, *10*(31), 2300401. https://doi.org/https://doi.org/10.1002/admi.202300401

Vondrak, J., Libich, J., Cech, O., Máca, J., & Sedlaříková, M. (2018). Supercapacitors: Properties and applications. *Journal of Energy Storage*. https://doi.org/10.1016/J.EST.2018.03.012

Wang, R., Yao, M., & Niu, Z. (2020). Smart supercapacitors from materials to devices. *InfoMat*, *2*(1), 113-125. https://doi.org/https://doi.org/10.1002/inf2.12037

Wibawa, P. J., Nur, M., Asy'ari, M., & Nur, H. (2020). SEM, XRD and FTIR analyses of both ultrasonic and heat generated activated carbon black microstructures. *Heliyon*, *6*(3), e03546. https://doi.org/https://doi.org/10.1016/j.heliyon.2020.e03546

Yao, M., Zhao, X., Jin, L., Zhao, F., Zhang, J., Dong, J., & Zhang, Q. (2017). High energy density asymmetric supercapacitors based on MOF-derived nanoporous carbon/manganese dioxide hybrids. *Chemical Engineering Journal*, *322*, 582-589. https://doi.org/https://doi.org/10.1016/j.cej.2017.04.075

Yu, L., Zhu, B., Yu, J., & Qiao, K. (2022). Preparation and Application Prospect of Activated Carbon Fiber Catalysts from Smart City Condition. *Procedia Computer Science*, *208*, 494-500. https://doi.org/https://doi.org/10.1016/j.procs.2022.10.068

Zhang, J., Zhou, J., Wang, D., Hou, L., & Gao, F. (2016). Nitrogen and sulfur codoped porous carbon microsphere: a high performance electrode in supercapacitor. *Electrochimica Acta*, *191*, 933-939. https://doi.org/https://doi.org/10.1016/j.electacta.2016.01.150

Zhang, L., Wang, N., Cao, P., Lin, M., Xu, L., & Ma, H. (2020). Electrochemical non-enzymatic glucose sensor using ionic liquid incorporated cobalt-based metal-organic framework. *Microchemical Journal*, *159*, 105343. https://doi.org/https://doi.org/10.1016/j.microc.2020.105343

Zhang, Y., Gao, Z., Song, N., & Li, X. (2016). High-performance supercapacitors and batteries derived from activated banana-peel with porous structures. *Electrochimica Acta*, *222*, 1257-1266. https://doi.org/https://doi.org/10.1016/j.electacta.2016.11.099

APPENDIX

LAB WORKS PHOTOGRAPHS

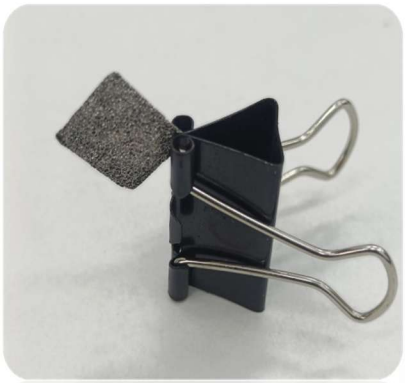

To Whom It May Concern

Corresponding author,

Dr. Tanka Mukhiya

Assistant Professor

Pulchowk campus

It is informed to you and concerned authors that the submitted article," **Metal Organic Framework Modification of Hemp Hurd Carbon for Supercapacitor" submitted in the Amrit Research Journal (ARJ) has been accepted for publication (Manuscript ID ARJ25-C1) on the date of April 20, 2025. We will inform you about its online available.**

Editor

Dr. Prakash Chandra Lohani

Amrit Research Journal

2025/04/21

13% Overall Similarity

The combined total of all matches, including overlapping sources, for each database.

Filtered from the Report

- Bibliography
- Quoted Text
- Cited Text
- Small Matches (less than 10 words)
- Abstract
- Methods and Materials

Match Groups

56 Not Cited or Quoted 13%
Matches with neither in-text citation nor quotation marks

0 Missing Quotations 0%
Matches that are still very similar to source material

0 Missing Citation 0%
Matches that have quotation marks, but no in-text citation

0 Cited and Quoted 0%
Matches with in-text citation present, but no quotation marks

Top Sources

9% Internet sources
10% Publications
0% Submitted works (Student Papers)

Integrity Flags

0 Integrity Flags for Review

No suspicious text manipulations found.

Our system's algorithms look deeply at a document for any inconsistencies that would set it apart from a normal submission. If we notice something strange, we flag it for you to review.

A Flag is not necessarily an indicator of a problem. However, we'd recommend you focus your attention there for further review.